Desalination and Water Treatment
www.deswater.com

doi:10.5004/dwt.2016.11079

61 (2017) 298–305
January

Numerical investigation on thermal non-equilibrium of condensation in the presence of non-condensable gas

Luopeng Yang*, Yan Yang, Hongyou Li, Chengyong Gu, Shengqiang Shen

Key Laboratory of Ocean Energy Utilization and Energy Conservation, Ministry of Education, Dalian University of Technology, Dalian, 116024, China, Tel. +86-411-84708460; Fax +86-411-84707963; email: yanglp@dlut.edu.cn

Received 17 April 2015; Accepted 20 June 2016

ABSTRACT

Condensation in the presence of non condensable gas (NCG), involving phase change and simultaneous heat and mass transfer progress, is common in many industries applications including nuclear, refrigeration, petrochemical, desalination and power industries. As there exists complex hydrodynamic interaction, heat and mass transfer between the vapor-NCG mixture and condensate for vapor condensation in present of NCG, a simulation model, based on the stagnant film model and gas-liquid two-phase conservation equations coupled with flow regime-dependent correlations, is developed to represent the heat, mass and momentum transfer at the gas-liquid inter-phase. A good agreement between the predictions and the available experimental data validates the accuracy of the two-phase numerical model. The effects of NCG concentration and vapor flow rate on the profiles of local void fractions, temperatures, pressures, heat and mass transfer coefficients are explored. The results show that compared with other parameters, NCG concentration is the key factor affecting the thermal interfacial non-equilibrium and condensation rate due to the fact that a small increase in NCG concentration drastically increase resistances of mass transfer at the gas side and heat transfer at both sides of gas and liquid. The heat transfer is controlled by both phases of condensate and gas through the quantitative analysis on the profiles of heat and mass transfer coefficients and temperatures at the gas-liquid interphase. Increasing the inlet gas mass flow rate contributes to reducing the adverse effect of NCG.

Keywords: Thermal non-equilibrium; Non-condensable gas; Condensation; Stagnant film model

1. Introduction

Condensation in the presence of NCG is common in many industries including nuclear, refrigeration, petrochemical, desalination, and power industries. As even very small amount of NCG in the bulk vapor significantly reduces heat transfer rates, it attracts much interest to investigate the mechanism of condensation in the presence of NCG.

A great deal of experimental and theoretical research has been done on the condensation process in the presence of NCG. The heat transfer deterioration caused by NCG is qualitatively understood [1,2]. The accumulation of NCG due to vapor condensation at the interface increases the diffusing resistance before vapor reaches the interface. For condensation in absence of NCG, the mass transfer at the interface is a combination of diffusion and convection. The study [3,4] concentrated on the liquid–side heat transfer while the flow field of vapor phase is not fully developed.

Most investigations focused on developing numerical methods or correlations to calculate the overall heat transfer coefficients of condensation in the presence of NCG. The effects of inlet NCG concentration, inlet mass flow rate and condensing pressure on vapor condensation in the presence of NCG have been experimentally and theoretically investigated in different flow configurations [5–9]. Although

*Corresponding author.

Presented at EuroMed 2015: Desalination for Clean Water and Energy Palermo, Italy, 10–14 May 2015. Organized by the European Desalination Society.

This work was supported by the National Natural Science Foundation of China (Grant No. 51576028 &51176019).

some investigations verified their predicted data in a good agreement with their experimental data, their correlations constrain in specific conditions and do not work on all the gas-liquid flow regimes. Besides, the hydrodynamics of gas phase, which varies significantly along the axial direction, affects the liquid phase hydrodynamics by the interfacial heat, mass and momentum transfer. As a result, the correlations [10–15] cannot be directly applied to condensation in the presence of NCG. The methods of degradation factor method [7] and diffusion layer theory [16,17], which are based on simplified assumptions and empirically adjust scale factors, can not fully represent the complex physical phenomena.

As thermal non-equilibrium between the two phases is an important characteristic of condensation in the presence of NCG, some investigators [18,19] have empirically correlated the thermal non-equilibrium with the overall heat transfer coefficients, and few work has been done to investigate the relationship between the local thermal non-equilibrium and local heat transfer coefficients. In addition, little attention has been given to quantitatively investigate on the thermal non-equilibrium at the gas-liquid inter-phase of vapor condensation with NCG although this thermal non-equilibrium is the key driving force of heat transfer.

Ren and Zhang [20,21] conducted an experimental investigation on condensation of a steam-air mixture inside a horizontal tube. Correlations based on Liao's modified diffusion layer theory were developed to estimate overall and local heat transfer coefficients. Their research on specific condensation with relatively high inlet NCG concentrations varying from 10 to 40% does not work on most condensation processes in industry. Much research has been done to measure void fraction in a gas-liquid two-phase flow [22–25] due to its importance in describing two-phase flow regimes.

In order to deeply understand the mechanism of vapor condensation in the presence of NCG, a simulation model, based on the gas-liquid two-phase conservation equations and the stagnant film model coupled with flow regime-dependent correlations, is developed. Thermal non-equilibrium between the gas and liquid phase are taken into account in the model. The profiles of local temperatures of two phases and the inter-phase, partial pressure and NCG concentrations, void fraction, liquid and gas sides heat and mass transfer coefficients are predicted along the tube length.

2. Mechanistic models

2.1. Stagnant film model

The stagnant film model [26,27] is an engineering method for calculating the heat and mass transfer processes. It's assumed that a quasi-steady stagnant vapor-NCG film resides adjacent to the gas-liquid inter-phase, that the mixture film separates the liquid-gas inter-phase from the bulk gas, and that the heat and mass transfer is driven by diffusion through the mixture film.

A schematic of the liquid-gas inter-phase in the condensation with NCG is shown in Fig. 1. Energy conservation at the interface is given as

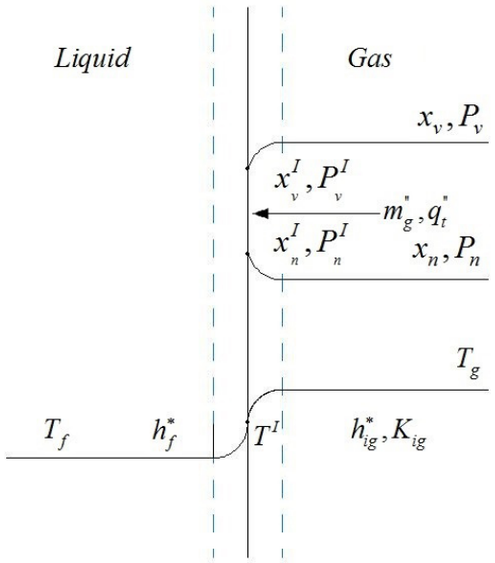

Fig. 1. Gas-liquid inter-phase of vapor condensation in the presence of NCG.

$$q_t'' = h_{if}^*(T^I - T_f) = h_{ig}^*(T_g - T^I) + m_c'' h_{fg} \tag{1}$$

The gas and liquid sides heat transfer coefficients accounting for the effect of mass transfer [27] are given as

$$h_{ig}^* = \frac{m_g'' C_{pv}}{\exp(-\frac{m_g'' C_{pf}}{h_{if}}) - 1} \tag{2}$$

$$h_{if}^* = \frac{m_g'' C_{pf}}{\exp(-\frac{m_g'' C_{pf}}{h_{if}}) - 1} \tag{3}$$

The condensation mass flux at the interface considering the suction effect of mass transfer, m_c'', is written as

$$m_c'' = -m_g'' = -\frac{\Gamma_g}{a''} = -K_{ig} \ln(\frac{x_n}{1 - x_v^I}) \tag{4}$$

The vapor mass fraction at the interface, x_v^I, is calculated as

$$x_v^I = \frac{X_v^I M_v}{X_v^I M_v + (1 - X_v^I) M_n} \tag{5}$$

where

$$X_v^I = \frac{P^s(T^I)}{P} \tag{6}$$

2.2. Gas-liquid two-phase conservation equations

The main assumptions are given as follows:

The flow with a uniform cross-section is steady and one-dimensional. The gas phase is a well-mixed mixture of NCG and vapor.

The gas-liquid mixture mass conservation can be written as

$$\frac{\partial}{\partial z}[\rho_f U_f(1-\alpha)+\rho_g U_g \alpha]=0 \tag{7}$$

The liquid mass conservation is given as

$$\frac{\partial}{\partial z}[\rho_f U_f(1-\alpha)]=a_i''' m_c'' \tag{8}$$

The NCG mass conservation equation is

$$\frac{\partial}{\partial z}[\rho_g U_g \alpha x_n]=0 \tag{9}$$

The momentum conservation equation for the vapor-NCG mixture is

$$\begin{aligned}&\rho_g \alpha U_g \frac{dU_g}{dz}=-\alpha\frac{dP}{dz}-\rho_g g\alpha\sin\theta\\&-F_i-F_{WG}-a_i''' m_c''(U_i-U_g)-C_{VM}(U_g\frac{dU_g}{dz}-U_f\frac{dU_f}{dz})\end{aligned} \tag{10}$$

The liquid momentum conservation equation can be represented as:

$$\begin{aligned}&\rho_f(1-\alpha)U_f\frac{d(U_f)}{dz}=-(1-\alpha)\frac{dP}{dz}-\rho_f g(1-\alpha)\sin\theta\\&+F_i-F_{WL}+a_i''' m_c''(U_i-U_f)+C_{VM}(U_g\frac{dU_g}{dz}-U_f\frac{dU_f}{dz})\end{aligned} \tag{11}$$

The two-phase frictional pressure drop is calculated according to the correlations of Friedel [28]. The interfacial surface area per unit two-phase mixture volume, a_i''' , interfacial force term, F_i, and the virtual mass force term in the above momentum conservation equations, are highly flow regime-dependent.

The coefficient, C_{VM}, in the virtual mass force term is calculated [29]:

$$C_{VM}=\alpha(1-\alpha)C_a[(1-\alpha)\rho_f+\alpha\rho_g] \tag{12}$$

The mixture thermal energy conservation equation is:

$$\begin{aligned}&\frac{d}{dz}[\rho_f U_f(1-\alpha)h_f+\rho_g U_g \alpha h_g]\\&=[\alpha U_g+(1-\alpha)U_f]\frac{dP}{dz}-q_w''\pi D\end{aligned} \tag{13}$$

The interfacial force term, together with heat and mass transfer in gas-liquid two-phase flow, depends on the flow regimes. Void fraction, α, was used to determine the flow regimes [30–32] and correlations [33–36] are introduced to estimate heat and mass transfer in different flow regimes. The flow regimes of bubbly, churn-slug and annular flows are introduced for the closure of two-fluid conservation equations.

3. Results and discussion

The initial parameters listed in Table 1 are given by Toda and Hori's experiment [22]. Fig. 2 shows a comparison of void fractions between the predictions and available experimental results [22]. It can be seen that the predicted void fractions agree well with the data in these given tests. A good agreement proves that the model is appropriate to represent the condensation of gas-liquid two-phase involving different flow regimes.

The given parameters of following numerical simulations are listed in Table 2. Figs. 3 and 4 show the predicted void fractions along the tube at different inlet NCG concentrations. It is shown in Fig.3 that the void fractions are highly sensitive to the inlet NCG concentrations. At low inlet NCG concentration of 0.1%, the void fraction decreases dramatically along the tube. With an increase in the inlet NCG concentration, the void fraction reduces at a slower speed, which indicates that a small increase in NCG concentration can obviously slow the condensation rate. When the inlet mass fraction increases from 0.1% to 5%, the condensation rate decreases about 50–70%

Fig. 4 shows the comparison of the void fractions for Test 1 and 3. As is shown in Table 2 above, the inlet gas mass flow rate in Test 1 is bigger than in Test 3. At all inlet NCG concentrations in both tests, void fractions in Test 3 is higher than that in Test 1, which indicates that increasing the inlet gas mass flow rate could increase the condensation rate. Increasing the inlet gas mass flow rate could reduce the adverse effect of NCG on condensation rate in some degree. The positive effect of increasing the inlet gas flow rate is more obvious at a higher inlet NCG mass fraction as the NCG film thickness is more easily affected by the interfacial force between gas and liquid phase.

Figs. 5 and 6 show the predicted phasic and gas-liquid inter-phase temperature profiles along the tube at different inlet NCG concentrations in Test 1 and 2. As is shown in Figs. 5a and 6a for inlet NCG MF = 0.001, the gas phase temperature is almost the same as the interfacial tem-

Table 1
Parameter setting of Toda and Hori's experiments

Toda's test	$(T-T_{sat})_{in}$(K)	$(T-T_{sat})_o$(K)	α_o	$U_{f,in}$ (m s^{-1})	$U_{f,o}$ (m s^{-1})	$U_{g,o}$ (m s^{-1})
VF3	9	7.6	0.813	0.64	3.39	11.2
VF4	10.2	8.5	0.808	0.64	3.3	10.5
VF5	7.4	5.8	0.784	0.85	3.91	9.94
VF6	8.2	6.5	0.780	0.85	3.84	9.66

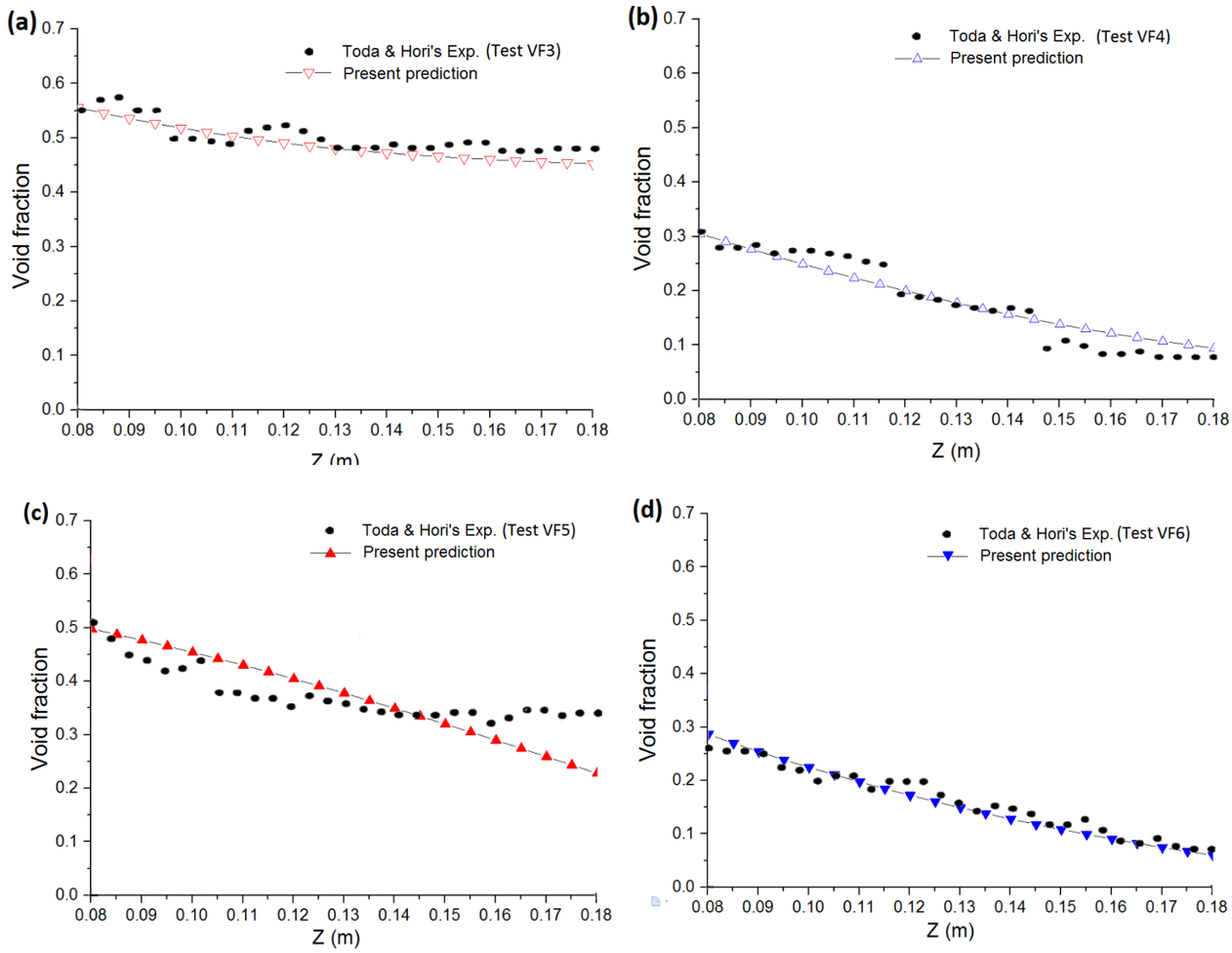

Fig. 2. Comparison of the predicting void fractions with experimental data.

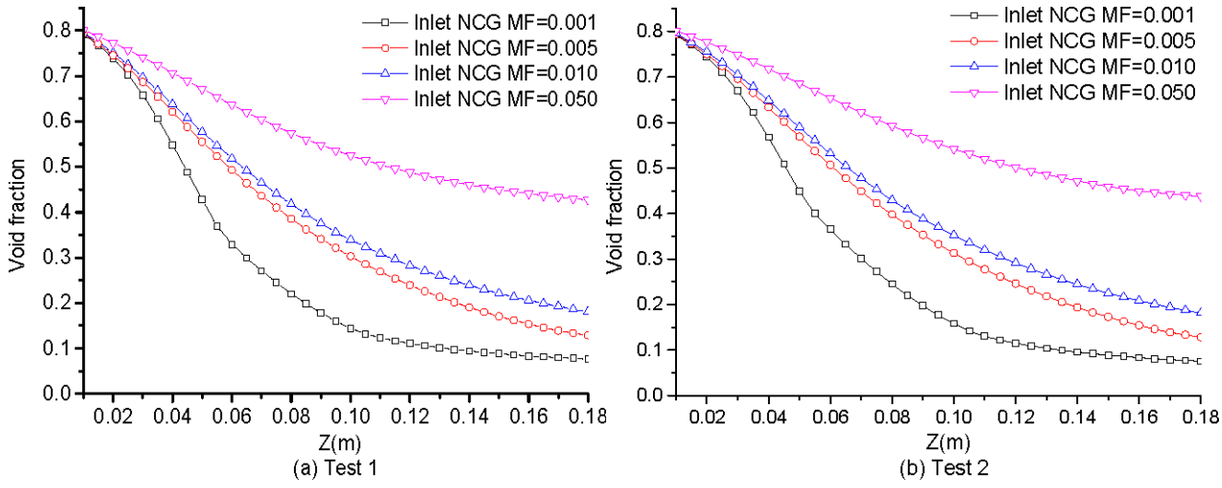

Fig. 3. Effect of inlet NCG concentrations on void fractions.

Table 2
Parameter setting of the simulation tests

Simulation test	α_o	$x_{n,in}$	$U_{f,o}$ (m s^{-1})	$U_{g,o}$ (m s^{-1})
1	0.813	0.1%, 0.5%, 1%, 5%	3.39	11.2
2	0.780	0.1%, 0.5%, 1%, 5%	3.84	9.66
3	0.813	0.1%, 0.5%, 1%, 5%	3.39	9

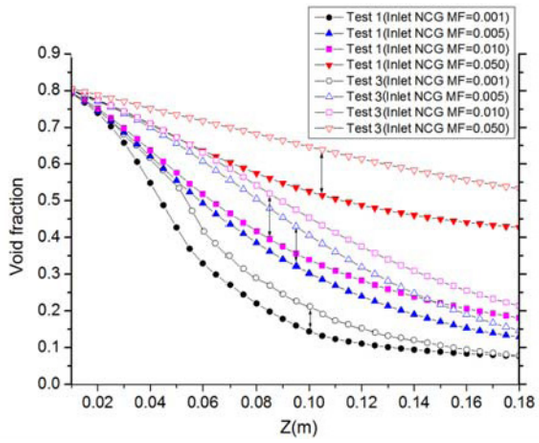

Fig. 4. Comparison of the variety of void fraction along the test tube in Test 1 and 3.

perature. The liquid phase temperature, which is lower than the gas and interfacial temperatures, obviously increases with the tube length, indicating an increase in thermal non-equilibrium between the two phases. With an increase in NCG concentrations, the temperature differences between the gas phase and the inter-phase increase while the temperature differences between the inter-phase and liquid phase decrease. Therefore, the thermal driving force decrease with increasing inlet NCG mass fraction.

Profiles of mass fraction at the inter-phase and gas side are shown in Fig. 7. It can be seen that the accumulation of NCG at the gas-liquid inter-phase during vapor condensation at the inter-phase and gas side explains the existence of thermal interfacial non-equilibrium and introduced mass transfer thermal resistance. The increasing thermal non-equilibrium between the gas phase and the inter-phase results in an increasing condensation heat and mass transfer resistance at the gas side.

Heat transfer coefficients for the sides of gas and liquid shown in Figs. 8, 9 decrease with increasing inlet NCG concentrations. Coupled with the decreasing thermal inter-phase non-equilibrium with the increasing NCG concentration, the heat flux at the gas-liquid inter-phase decreases. Thus void fractions along the tube length reduce at a slower speed in Figs. 3, 4. It's also found that the liquid-side heat transfer coefficients in Fig. 8 are more than the gas-side heat transfer coefficients. This is because the gas-side heat transfer includes

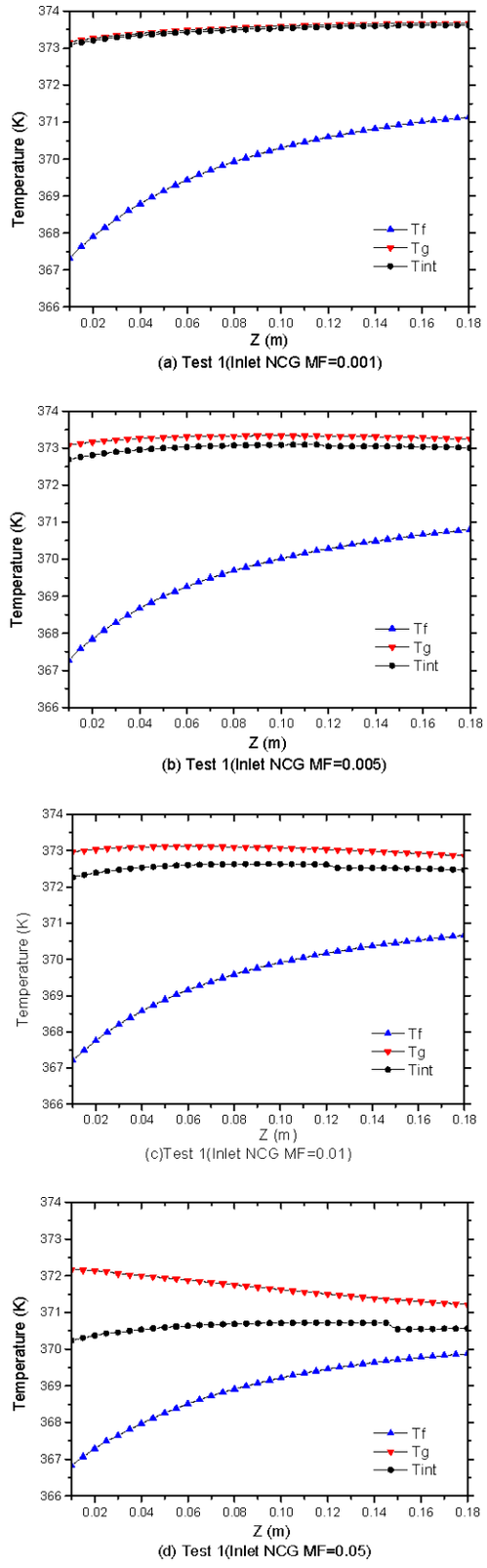

Fig. 5. Profiles phasic and interfacial temperatures along the tube inTest 1.

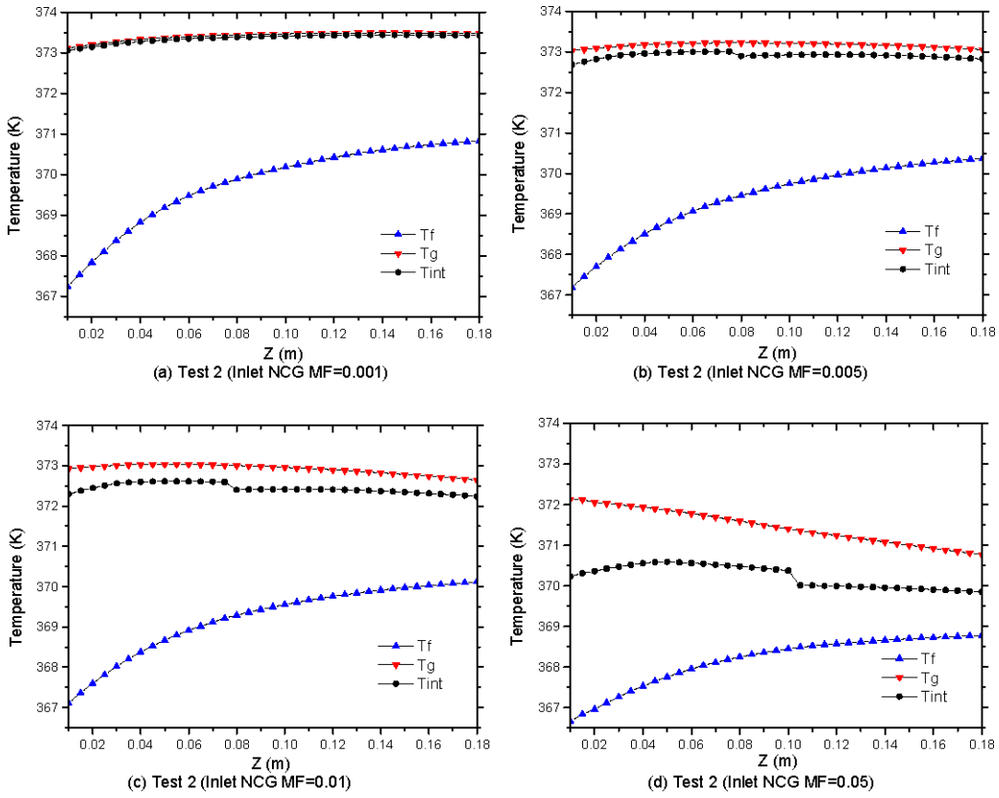

Fig. 6. Profiles phasic and interfacial temperatures along the tube in Test 2.

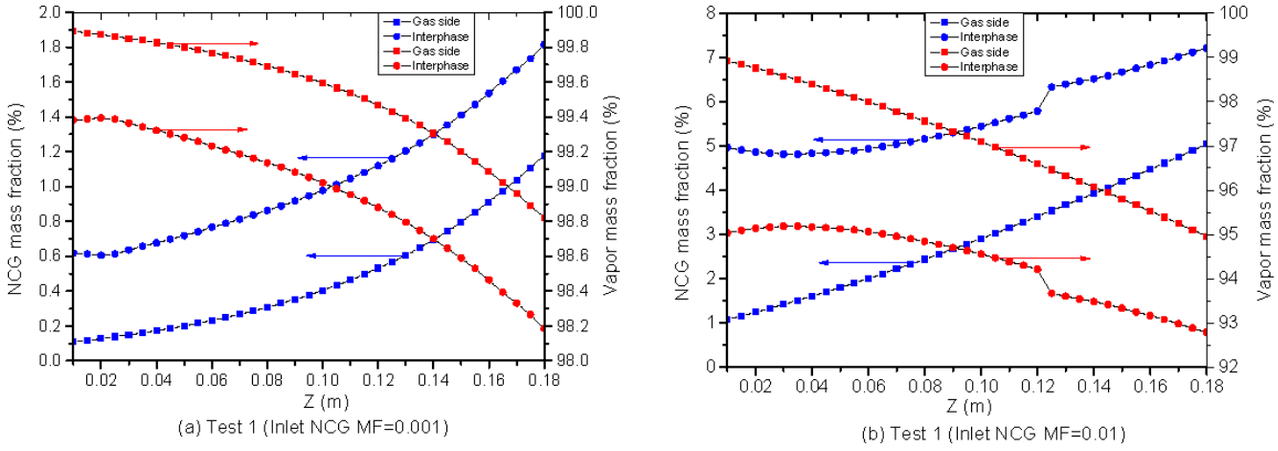

Fig. 7. Profiles of predicted gas-side and interfacial NCG and vapor mass fraction in Test 1.

latent heat and convective sensible heat transfer and the latent heat transfer weighs more the convective sensible heat transfer. When the inlet NCG mass fraction increases from 0.1% to 5%, the percentage of convective sensible heat transfer at the gas-side obviously increases from 0.002% to 0.3%, and the gas-side latent heat transfer coefficients decreases about 50%. Therefore, condensation in the presence of NCG is controlled by both the liquid phase and gas phase.

4. Conclusions

A simulation model, based on the gas-liquid two-phase conservation equations and stagnant film model coupled with flow regime-dependent correlations, is developed, and can adequately predict condensation in the presence of NCG in two-phase flow regimes.

The NCG concentration plays a key role in controlling the condensation rate as a very small increase in NCG con-

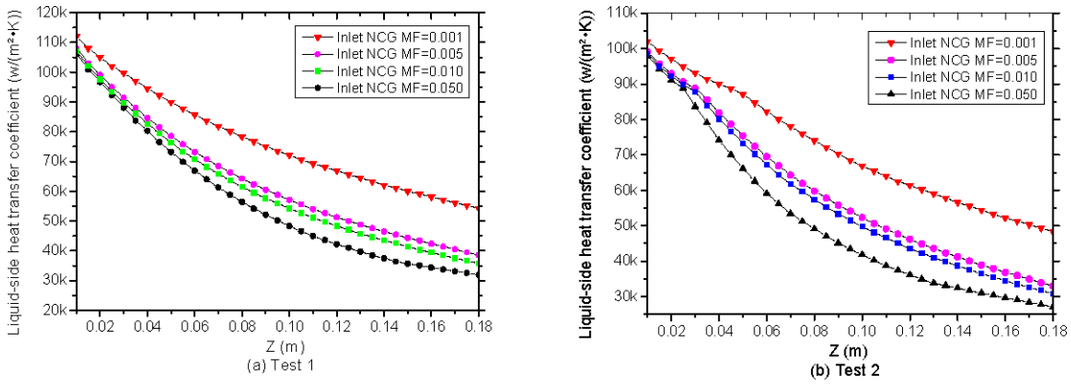

Fig. 8. Profiles of liquid-side heat transfer coefficient along the tube in Test 1 and 2.

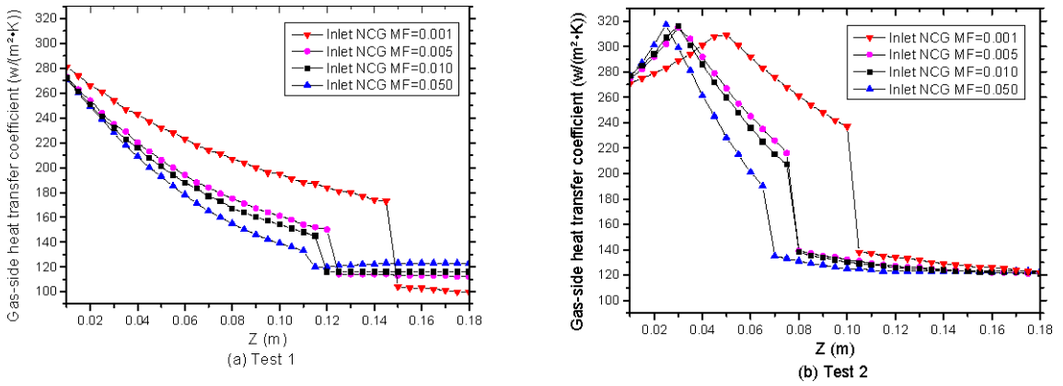

Fig. 9. Profiles of gas-side heat transfer coefficient along the tube in Test 1 and 2.

centrations significantly reduces the interfacial heat and mass transfer rates.

The quantitative analysis on the profiles of void fraction, temperature of both phases and the inter-phase, partial mass fraction and pressure of NCG and vapor, gas- and liquid-side heat transfer coefficient and gas-side mass transfer coefficient reveals heat and mass transfer mechanism of vapor condensation process in the presence of NCG.

A decrease in the heat transfer thermal driving force and heat transfer coefficient with increasing NCG concentrations results in decreasing heat flux and condensation rates.

Condensation in the presence of NCG is controlled by both the liquid phase and gas phase based on the profiles of local thermal interfaicial non-equilibrium and heat transfer coefficients. Increasing the inlet gas mass flow rate could reduce the adverse effect of NCG and this positive effect of increasing the inlet gas flow rate is more obvious at a higher given inlet NCG mass fraction.

Symbols

a″ — Specific interface area per unit mixture volume m^{-1}
Cp — Specific heat at the gas phase J $(kg{\cdot}K)^{-1}$
C — Dimensionless constant
D — Diameter m
F — Friction N
G — Gravitational constant m s^{-2}
h — Heat transfer coefficient W $(m^2{\cdot}K)^{-1}$
h_{fg} — Latent heat of vaporization J kg^{-1}
h^*_{ig} — The gas-side heat transfer coefficient at the interface W $(m^2{\cdot}K)^{-1}$
h^*_{if} — The liquid-side heat transfer coefficient at the interface W $(m^2{\cdot}K)^{-1}$
$\hat{h}$ — Specific enthalpy J kg^{-1}
K_g — Mass transfer coefficient kg $(m^2{\cdot}s)^{-1}$
M — Molar mass kg mol^{-1}
m''_g — Evaporation mass flux kg $(m^2{\cdot}s)^{-1}$
m''_c — Condensation mass flux kg $(m^2{\cdot}s)^{-1}$
P — Pressure N m^{-2}(Pa)
q″ — Total heat flux at the interface J $(m^2{\cdot}s)^{-1}$
T — Temperature K
U — Velocity m s^{-1}
X — Mass fraction
X — Mole fraction
Z — Axial coordinate m

Subscripts

In — inlet
I — interface

F — liquid
G — gas
N — NCG
O — outlet
S — saturation
T — total
V — vapor
VM — the visual mass
W — wall

Greeks

α — void fraction
ρ — density kg m^{-3}
θ — angle

References

[1] R. Benelmir, S. Mokraoui, A. Souayed, Numerical analysis of filmwise condensation in a plate fin-and-tube heat exchanger in the presence of non-condensable gases, Heat Mass Transfer, 45 (1990) 1561–1573.
[2] V. Dharma Rao, V. Murali Krishna, K.V. Sharma, P.V.J. Mohana Rao, Convective condensation of vapor in the presence of a non-condensable gases of high concentration in laminar flow in a vertical pipe, Int. J. Heat Mass Transfer, 51 (2008) 6090–6101.
[3] L. Zhang, H. Zheng, Y. Wu, Experimental study of a horizontal tube falling film evaporation and closed circulation solar desalination system, Renew. Energy, 28(8) (2003) 1187–1199.
[4] Z. Liu, Q. Zhu, Y. Chen, Evaporation heat transfer of falling water film on a horizontal tube bundle, Heat Trans.-Asian Res., 31(1) (2002) 42–55.
[5] Justin D. Talley, Ted Worosz, Seungjin Kim, John R. Buchanan Jr., Characterization of horizontal air-water two-phase flow in a round pipe part I: Flow visualization, Int. J. Multiphase Flow, 76 (2015) 212–222.
[6] Gianfranco Caruso, Damiano Vitale Di Maio, Heat and mass transfer analogy applied to condensation in the presence of noncondensable gases inside inclined tubes, Int. J. Heat Mass Transfer, 68 (2014) 401–414.
[7] S.Z. Kuhn, V.E. Schrock, P.F. Peterson, An investigation of condensation from steam-gas mixtures flowing downward inside a vertical tube, Nucl. Eng. Design, 177 (1997) 53–69.
[8] Y.A. Hassan, and S. Banerjee, Implementation of a non-condensable model in RELAP5/MOD3, Nucl. Eng. Design, 162 (1996) 281–300.
[9] Jun-De Li, CFD simulation of water vapour condensation in the presence of non-condensable gases in vertical cylindrical condensers, Int. J. Heat Mass Transfer, 57 (2013) 708–721.
[10] M.M. SHAH, A general correlation for heat transfer during film condensation inside pipes, Int. J. Heat Mass Transfer, 22 (1979) 547–556.
[11] D. Luo, Inter-phase Transfer Process in Cocurrent Two-Phase Channel Flow, Ph.D Thesis, Georgia Institute of Technology, 1995.
[12] V.P. Carey, Liquid-vapor phase change phenomena, Hemisphere, New York, 1992.
[13] M.S. Al-Johani, A Three-Dimensional Mechanistic Model of Steam Condensers Using Porous Medium Formulation, Ph.D Thesis, Georgia Institute of Technology, 1996
[14] S.B. Al-Shammari, D.R. Webb, P. Heggs, Condensation of steam with and without the presence of non-condensable gaseses in a vertical tube, Desalination, 169 (2004) 151–160.
[15] R. Semiat, and Y. Galperin, Effect of non-condensable gasses on heat transfer in the tower MED seawater desalination plant, Desalination, 140 (2001) 27–46.
[16] S.M. Ghiaasiaan, A.T. Wassel, C.S. Lin, Direct contact condensation in the presence of noncondensable in OC-OTEC condensers, J Solar Energy Eng., 113 (1991).
[17] T. Kageama, P.F. Peterson, V.E. Schrock, Diffusion layer modeling for condensation in vertical tube with noncondensable gases, Nucl. Eng. Design, 141 (1993) 289–302.
[18] D.F., Othmer, The condensation of steam, Ind. Eng. Chem., 21(1929) 576–583
[19] I.Y. Chen, Heat transfer analysis of a falling-film horizontal tube evaporator, Ph.D thesis, the University of Wisconsin-Milwaukee, 1984.
[20] B. Ren, L. Zhang, H. Xu, J. Cao, Z.Y. Tao, Experimental study on condensation of steam/air mixture in a horizontal tube, Experim. Thermal Fluid Sci., 58 (2014) 145–155.
[21] B. Ren, L. Zhang, J.Cao, H. X, Z.Y. Tao, Experimental and theoretical investigation on condensation inside a horizontal tube with noncondensable gas, Int. J. Heat Mass Transfer, 82 (2015) 588–603.
[22] S. Toda, and Y. Hori, Characteristics of two-phase condensing flow by visualization using computed image processing, Nucl. Eng. Design, 141 (1993) 35–46.
[23] E. Nazemi, S.A.H. Feghhi, G.H. Roshani, R. Gholipour Peyvandi, and S. Setayeshi, Precise void fraction measurement in two-phase flows independent of the flow regime using gamma-ray attenuation, Nucl. Eng. Technol., 48 (2016) 64–71.
[24] G.H. Roshani, E. Nazemi, S.A.H. Feghhi, S. Setayeshi, Flow regime identification and void fraction prediction in two-phase flows based on gamma ray attenuation, Measurement, 62 (2015) 25–32.
[25] J. Jia, A. Babatunde, M. Wang, Void fraction measurement of gas–liquid two-phase flow from differential pressure, Flow Measurem. Instrument., 41 (2015) 75–80.
[26] R.B. Bird, W.E. Stewart, E.N. Lightfoot, Transport Phenomena, John Wiley and Sons, New York, 1960.
[27] D.K. Edwards, V.E. Denny, A.F. Mills, Transfer Processes, Hemisphere, New York, 2nd ed., 1979.
[28] L. Friedel, Druckabfall bei der Strömung von Gas/Dampf-Flüssigkeits-Gemischen in Rohren, Chem. Ing. Tech. 50 (1978) 167–180.
[29] V.H. Ransom, R.J. Wagner, J.A. Trapp, L.R. Feinaner, G.W. Johnsen, D.M. Kiser, R.A Riemke, RELAP5/MOD2 code manual, volume 1: Code structure, systems models, and solution methods, NUREG/CR-4312, U.S. Nuclear. Regulatory. Commission, 1985.
[30] K.E. Carlson, et. al., RELAP5/MOD3 code manual vol. 1, 2, 3, NUREG/CR-5535, EGG-2596, U.S. Nuclear Regulatory commission, 1990.
[31] M. Ishii, Zubber, Drag coefficient and relative velocity in bubbly droplet or particular flows, AIChE J., 25 (1979) 848–855.
[32] K.O. Passamehmetoglu, et al., TRAC-PF1/MOD2 theory manual, U.S. Nuclear Regulatory Commission Report (Draft), 1990.
[33] G.B. Wallis, One-dimensional two-phase flow, New York, McGraw-Hill, 1969.
[34] A.T. Wassel, A.F. Mills, D.C. Bugby, Analysis of radionuclides retetion in water pools, Nucl. Eng. Design, 90 (1985) 87–104.
[35] R. Kronig, J. C. Brink, On the theory of extraction from falling droplets, Appl. Scient. Res. A2, (1951) 142–154.
[36] H. J. Richter, Separation and two-phase flow model: application to critical two-phase flow, Int. J. Multiphase flow, 9 (1983) 511.